JOURNAL OF MATERIALS SCIENCE 23 (1988) 1547–1552

Structure and microhardness of laser-hardened 1045 steel

M. RIABKINA-FISHMAN, J. ZAHAVI
Israel Institute of Metals, Technion, Haifa, Israel

Observations are reported on the effect of continuous CO_2 laser irradiation on the structure and microhardness of AISI 1045 steel. In the case of isolated beam passes, martensite formed in the melt zone and in former pearlite regions of the austenitization zone exhibits very high Vickers hardness values (HV 750 and 900, respectively). However, in the case of contiguous or partly overlapping passes a zone of tempered martensite with hardness down to HV 400 forms behind each pass, thus resulting in a seesaw hardness distribution across the processed surface. It has been found that a drastic decrease in the size of the laser-affected region occurs when the beam power density exceeds a certain threshold level.

1. Introduction

Laser beam processing has been found to produce surface hardening in carbon and low-alloyed steels as a result of local heating, above or below the melting point, of a thin surface layer followed by rapid resolidification and/or self-quenching (see for example [1]). Available information relating the conditions of laser processing to the changes in structure and hardness is largely confined to the case of an individual laser beam exposure, whether in the form of a pulse spot or of a single pass of a continuous beam [2–4]. Although the structures produced over extended surfaces processed by a series of successive passes are of the highest practical interest, only limited data (concerning mainly residual stresses in the surface layer) have been reported [5–9].

In this investigation we have studied the structure and microhardness of the laser-affected region produced in AISI 1045 steel by a single beam pass, as well as by successive passes with varying degrees of overlapping.

2. Experimental procedure

The study was conducted on 5 mm thick specimens cut in the transverse direction from a 1 in. (25 mm) rod of commercial AISI 1045 steel in as-received condition. The specimen surface was ground down to 320 grit paper. Irradiation was carried out by means of a continuous CO_2 laser with maximum power 900 W; the beam was formed by a lens with focal distance 92.5 mm, and its diameter was 200 μm at the focal distance. To protect the lens against contamination and overheating and to minimize specimen oxidation under the beam, a flow of argon or nitrogen at excess pressure 1 atm directed at the irradiated surface was used. The specimens were fixed on a rotating table, and the transverse velocity of the beam over the specimen surface could be regulated by changing the rotation speed of the table. Provision for step-shifting of the table enabled the specimen to be advanced a certain distance in the radial direction with each revolution of the table, whereby a series of equidistant beam passes could be obtained.

Irradiation parameters were varied by changing the laser power (in the range of 300 to 900 W), the distance of the specimen surface from the focal plane (up to 3 mm), and the specimen velocity (in the range of 4 to 90 cm sec^{-1}). In addition, antireflection coatings (manganese phosphate, chromium powder – both with an organic binder –, a conducting carbon coating or an oxidation film produced by 20% orthophosphoric acid) were applied to the specimens in some experiments.

The structures produced by the processing were analysed by means of optical microscopy, scanning electron microscopy (SEM) and X-ray diffractometry. Prior to the preparation of cross-sectional samples for metallographic observation, a layer of nickel coating was electroplated on some specimens. The Vickers hardness (HV) was measured with a Matsuzawa DMN2 microhardness tester under a 50 g load.

3. Results and discussion

We first present and discuss the structure and hardness of the laser-hardened region in the case of a single (or isolated) pass and then those of an extended surface area processed by series of closely spaced or partially overlapping passes.

3.1. Single-pass laser beam irradiation

A low-magnification SEM image presented in Fig. 1a shows the free surface of a specimen with two tracks of laser irradiation. In appearance, the tracks resemble a weld seam and have a well-pronounced ripple structure. The dendrite structure of the ripples, revealed under higher magnification (Fig. 1b), indicates that melting has taken place in the region.

A typical structure of the laser-affected region, as revealed by optical microscopy and SEM in a transverse cross-section, is presented in Figs 2 and 3. The initial structure of 1045 steel consists of dark regions of pearlite (exhibiting a plate-like structure in the

0022–2461/88 $03.00 + .12

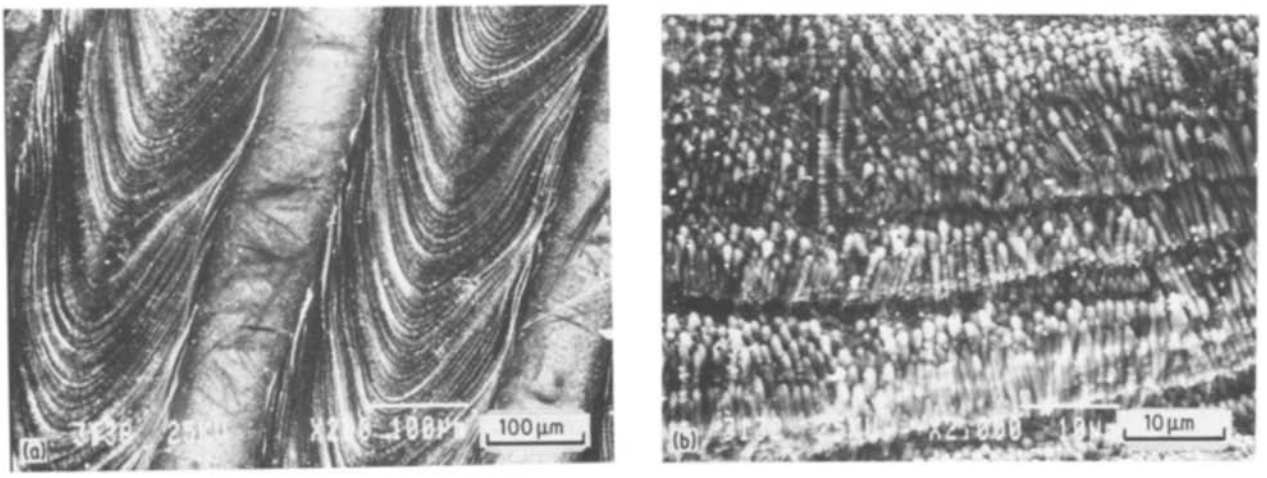

Figure 1 (a) SEM image of two laser beam passes on the surface of AISI 1045 steel: (b) enlarged view showing dendrite structure of ripples. Irradiation conditions: beam power 700 W, traverse velocity 40 cm sec^{-1}, uncoated specimen.

SEM image) and white grains of ferrite. The laser-affected region consists of two distinct zones already described in the literature [3], namely a melt zone surrounded by an austenitization zone. (Although the latter is referred to in the literature as a "heat-affected zone" we prefer a more specific term indicating explicitly that the temperature increase in this zone was sufficient for austenitization to take place.) The melt zone has a dendrite structure revealed by both optical metallography and SEM. The austenitization zone has a duplex structure with former pearlite and ferrite regions readily recognizable within it. However, the former pearlite regions show a much lower etchability than the original pearlite and even lower than the melt zone. In the SEM image former pearlite regions have a rather smooth appearance but the plate-like structure typical of pearlite is still discernible in some places in Fig. 3. The most interesting feature of the former ferrite grains within the austenitization zone observed in Fig. 2 is that their boundaries become fuzzier on approaching the melt-zone boundary. As a result, smaller grains situated in the inner part of the austenitization zone appear as contourless light spots.

Though no morphological features of martensite transformation were revealed by optical or scanning electron microscopy, the presence of martensite was confirmed by an X-ray diffraction pattern taken from the surface swept by a series of parallel passes; the presence of some amounts of retained austenite was also found.

There is no systematic variations of microhardness within the melt zone. The values observed are in the range of HV 730 to 760 when argon flow is used and HV 850 over the whole depth of the melt zone if nitrogen is used. It should be noted that no effect of nitrogen on hardness is observed in coated specimens, but the chromium coating itself increases the hardness of the melt zone up to HV 925.

Hardness values obtained within the austenitization zone depend primarily on whether the measurements are taken in the regions of former ferrite or pearlite. In former pearlite regions the hardness is higher than in the melt zone in the case of argon flow and reaches HV 900; at the former ferrite grains the hardness drops to HV 250. For comparison, outside the laser-affected region pearlite and ferrite have hardness values of HV 300 and HV 180, respectively, whereas the same steel after austenitization and conventional hardening by water quenching has hardness HV 710.

The uniform hardness within the melt zone is

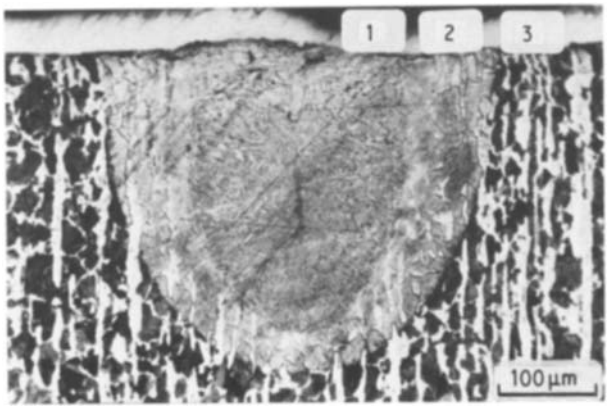

Figure 2 Optical micrograph showing typical cross-sectional structure of single laser-beam pass: (1) melt zone, (2) austenitization zone, (3) unaffected ferrite–pearlite substrate. Irradiation conditions: 300 W, 4 cm sec^{-1}, uncoated specimen.

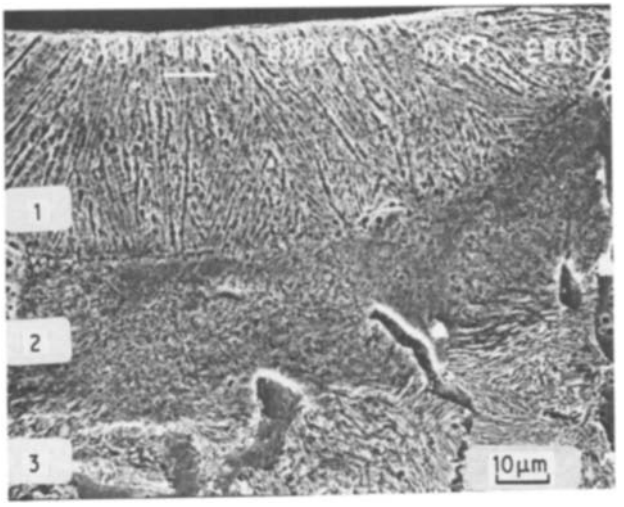

Figure 3 SEM image of cross-section of single laser-beam pass: (1) melt zone (2) austenitization zone, (3) unaffected ferrite–pearlite substrate. Irradiation conditions: 700 W, 40 cm sec^{-1}, uncoated specimen.

indicative of a uniform carbon distribution achieved during the laser-induced remelting, as a result of a vigorous agitation of molten material within the melt pool [10]. The higher hardness of the martensite formed in the melt zone can be attributed to the very high cooling rate achieved in this case.

As evidenced by the distinct contrast between former ferrite and pearlite regions within the austenitization zone, the austenite condition within this zone was too short-lived for appreciable long-range carbon diffusion to take place, and only the onset of this process could be traced in the vicinity of the melt zone, due to the higher temperatures (approaching the melting point) which prevailed there. As a result, the austenite formed during heating had a very low carbon content in the former ferrite regions and one close to the eutectoid level (0.8% C) in the former pearlite regions. The higher carbon content in the latter case seems to account for the higher hardness of the martensite formed in these regions compared with the martensite within the melt zone. As for the higher hardness of the former ferrite regions within the austenitization zone compared with that of the substrate ferrite, it has been reported that under high cooling rates produced by laser processing, martensite-type transformation also takes place in Armco iron resulting in hardness values of HV 380 in the melt zone [11] and of HV 250 when no melting occurs [12].

3.2. Overlapping laser irradiation passes

In most industrial applications of laser hardening, the surface to be processed is too large to be covered with a single pass. One of the feasible ways to produce a laser-hardening effect on an extended surface is by sweeping it with a series of successive passes with the workpiece advanced after each pass.

We have studied the structure and hardness of surface layers produced by this technique at various degrees of overlapping between successive passes. The results are illustrated by Figs 4a to c, which refer to a manganese-phosphate-coated specimen processed by six passes of a 700 W laser beam, with the advance of the specimen between passes being 300, 200 and 100 μm, respectively, and by Figs 5a and b which refer to an uncoated specimen swept by a series of passes displaced by 100 μm with beam power 900 and 700 W, respectively.

In spite of the fact that all irradiation parameters such as power, transverse velocity and specimen distance from the focal point were kept constant during each series of passes, in some cases, as can be seen in Figs 4 and 5a, the size of the laser-affected region was largest at the first pass and then decreased, to a greater or lesser extent, with each subsequent pass. We have found that this effect appears only when the beam power exceeds a certain threshold level that depends on other experimental conditions. For example, for an uncoated specimen and traverse speed 30 cm sec^{-1} the effect is very strong when a 900 W beam is used (Fig. 5a) and vanishes at beam powers of 800 W and less. The observed attenuation of the laser-induced effect during the first three passes was so drastic that, rather paradoxically, the subsequent depth of the laser-affected region was much smaller than the fairly steady depth produced under similar experimental conditions by a beam of only 700 W (Fig. 5b). Anti-reflection coatings, by increasing the fraction of beam power absorbed by the specimen, reduce the threshold

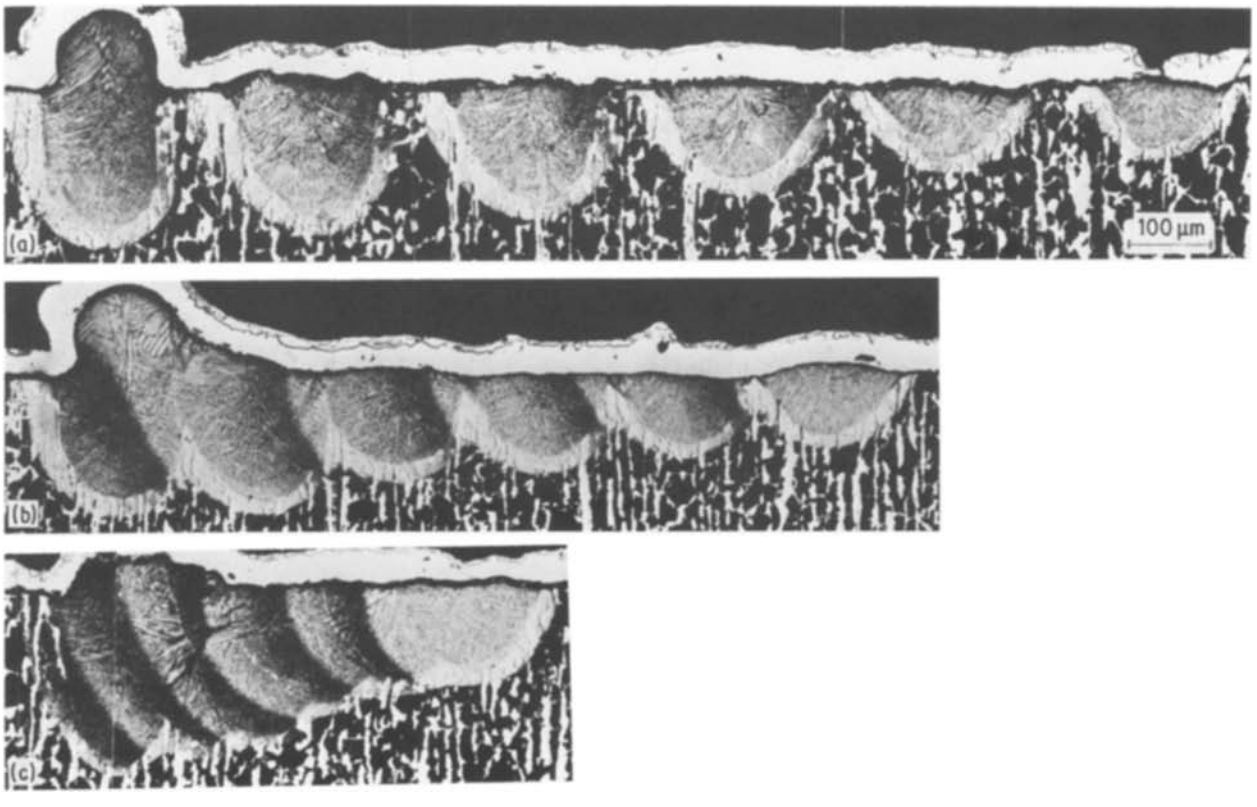

Figure 4 Cross-section of specimen processed from left to right by a series of six equidistant passes. Specimen advance between passes is (a) 300 μm, (b) 200 μm, (c) 100 μm. Irradiation conditions: 700 W, 40 cm sec^{-1}, manganese phosphate coating.

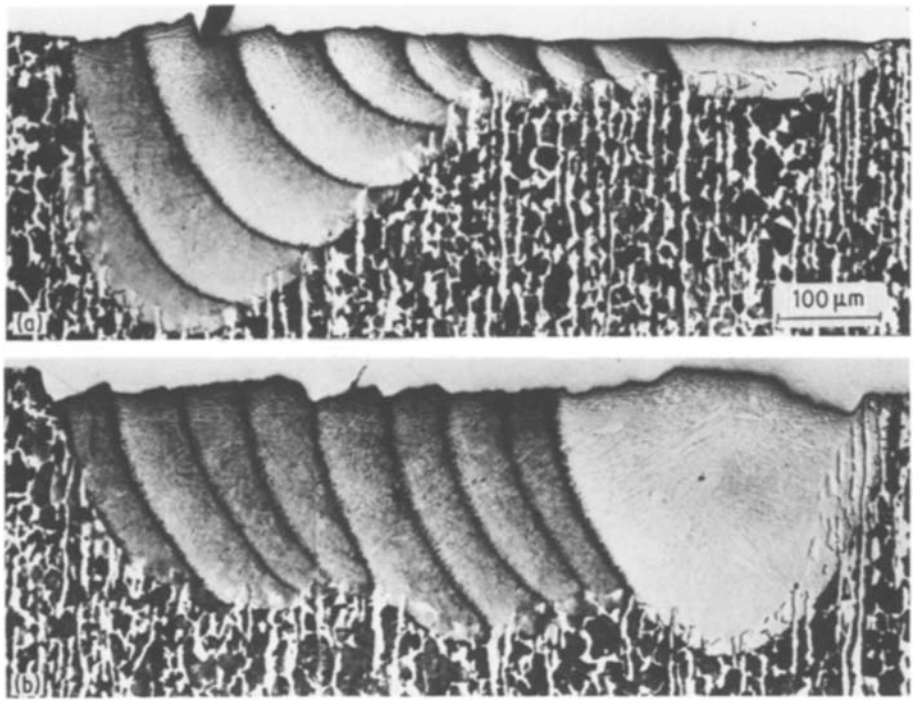

Figure 5 Cross-section of specimen processed, from left to right, by series of passes 100 μm apart. Irradiation conditions: (a) 900 W, (b) 700 W; 30 cm sec^{-1}; uncoated specimen.

level and the effect is already quite pronounced at 700 W (Fig. 4).

In our opinion, this phenomenon can be attributed to the beam attenuation caused by the absorbing plasma that forms near the irradiated surface and propagates along the direction of the beam [13]. This effect, often referred to as a laser-supported absorption, appears in the case of excessive metal heating and evaporation and its initiation is characterized by a definite threshold value of laser power density. It should be noted, however, that in our case the threshold value of energy density was at least one order of magnitude lower than that given by Ready [13].

Another unusual phenomenon observed under conditions of high power densities is the formation of large-scale undulations of the solidified surface, with the amplitude comparable to the depth of the melt zone (Fig. 6). These undulations appear only at the initial stage of irradiation while a large-depth melt zone is produced; later a rather smooth transition to the regular ripple morphology occurs as can be seen in the second pass in Fig. 6. In transverse cross-section these undulations exhibit a regular semicircular shape (see first passes in Figs 4a and b).

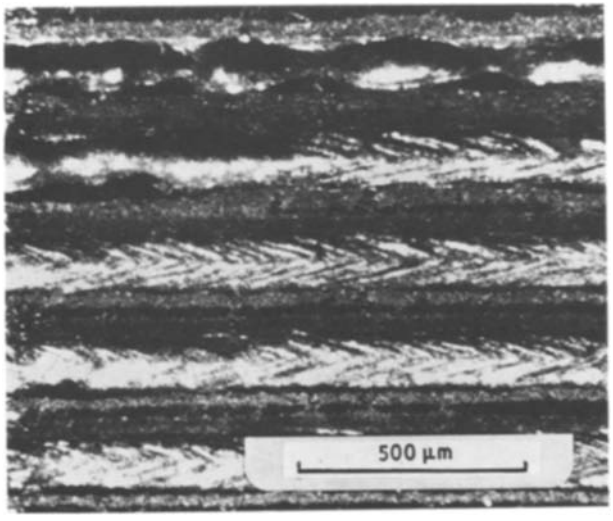

Figure 6 Optical photograph of specimen surface processed, from top to bottom, by a series of equidistant passes 450 μm apart. Note transition from large-scale undulations to ripple structure that occurs in the second pass. Irradiation conditions: 700 W, 30 cm sec^{-1}, manganese phosphate coating.

Fig. 4 brings out the structural changes undergone by the laser-affected region as the overlapping of the passes increases. When the austenitization zones of adjacent passes are in contact (Fig. 4a) the only change is a gradual increase in etchability of both the melt and, especially, the austenitization zones on approaching the boundary of the next pass in the series; this effect becomes more pronounced as overlapping increases (Fig. 4b). In the case of a substantial overlapping (Figs 4c and 5) high etchability characterizes the whole beam-affected region, except the area of the last pass. However, an appreciable contrast still remains at the outer boundaries of all austenitization zones.

Another change concerns the structure of the austenitization zone. The part of the zone that overlaps the melt zone of the preceding pass inherits its existing dendrite structure and can be distinguished from the latter only owing to its lower etchability (see Figs 4b and c). The "primary" duplex-structure austenitization zone survives only where there is no overlapping between it and the melt zones of the preceding or subsequent passes. As a result, the surface layer formed by a series of overlapping passes appears, at first glance, as a continuous melt zone showing a dendrite structure surrounded by a cusped band of the continuous duplex-structure austenitization zone.

As regards the influence of overlapping on the hardness distribution, we first consider the case of two overlapping passes illustrated by Fig. 7a. In the scheme in Fig. 7b we use numbers 1 and 2 to denote, respectively, the processes of melting and austenitization as well as to designate the "primary" melt and

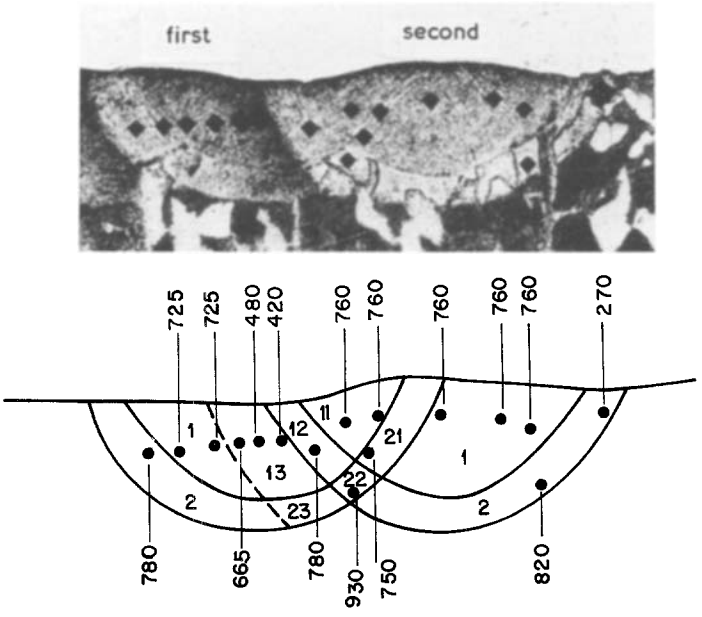

Figure 7 Structure and hardness distribution observed in the case of two partially overlapping passes: (1) primary melt zone, (2) primary austenitization zone, (1 1) double-melted zone, (1 2) austenitized melt zone, (2 1) remelted austenitization zone, (2 2) double-austenitization zone, (1 3) tempered melt zone, (2 3) tempered austenitization zone.

austenitization zones. By using the same symbols, the area of overlapping in Fig. 7 can be considered as composed of four zones designated as (1 1) double melt zone, (1 2) zone of melting followed by austenitization, (2 1) remelted austenitization zone, and (2 2) double austenitization zone.

As hardness measurements in this and other specimens have shown, the double-melted Zone 1 1 as well as the remelted austenitization Zone 2 1 have the same hardness as the primary melt Zone 1. Zone 1 2 shows, in this specimen as well as in others, a slight but steady increase in hardness over the melt zone. And, finally, the highest hardness is observed in the double austenitization Zone 2 2.

However, the most important change in hardness occurs within Zones 1 and 2 of the first pass: hardness decreases on approaching the boundary of the second pass and in some cases values as low as HV 400 have been measured in the vicinity of the boundary. This sharp decline in hardness (accompanied by an increase in etchability) is due to a tempering effect produced by each beam pass on the martensite of the earlier formed melt and austenitization zones. Quite obviously, the effect was strongest near the austenitization zone boundary of the superimposed pass where the temperature, albeit for a short time, approached the austenitization level. Assigning the number 3 to the tempering effect produced by the laser beam beyond the boundary of the austenitization zone, we have designated in Fig. 7b as 1 3 and 2 3 the regions of tempered martensite within the melt and austenitization zones, respectively.

As hardness measurements have shown, the tempered zone with hardness below HV 700 was 65 μm wide when the melt zone was 165 μm wide and reached 100 μm when the latter was 245 μm, i.e. the width of the tempered zone is about 40% of that of the melt zone. At such a ratio, even if melt zones of adjacent passes are merely in contact, about one-third of the hardened surface would be tempered to a greater or lesser extent. Due to the tempering effect, high hardness values typical of laser hardening cannot be achieved over the whole surface covered by a series of overlapping passes. Instead, there is a periodic hardness distribution whose features depend on the degree of overlapping. Fig. 8 presents schematically the hardness distribution pattern in the cases when the melt zones overlapped by 1/3, 1/2 and 3/4 of their width. It can be seen that with a high degree of overlapping (Fig. 8c) corresponding approximately to the case of Fig. 5b, the whole hardened layer turns into tempered martensite with a periodic hardness pattern reflecting the distribution of tempering temperatures.

An attempt to minimize tempering effect by avoiding overlapping even between austenitization zones

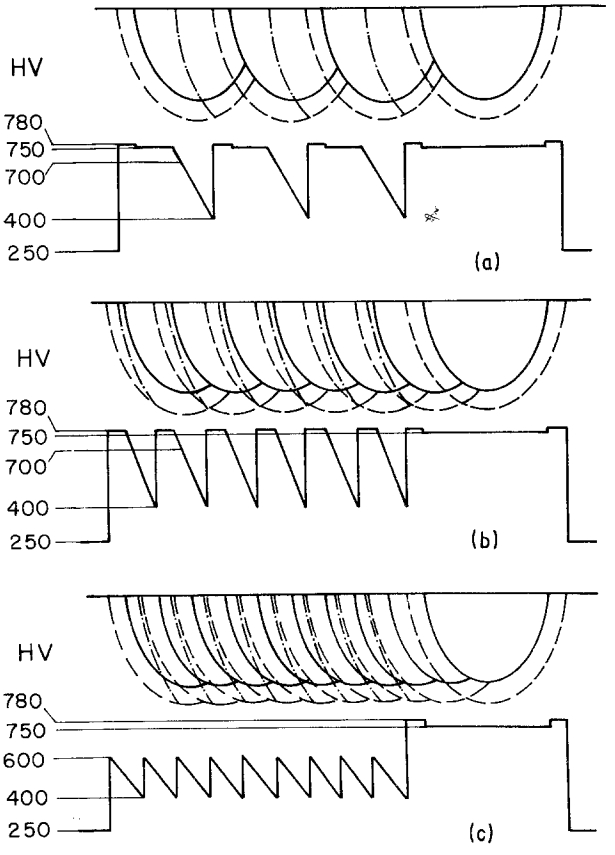

Figure 8 Examples of hardness distribution pattern across specimen surface covered by a series of equidistant passes overlapping by (a) 1/3, (b) 1/2 and (c) 3/4 of their melt-zone width.

leads, as can be seen in Fig. 4a, to the depth of hardened layer being very shallow where austenitization zones meet. In addition, low-hardness regions of former ferrite within austenitization zones can emerge at the surface in this case. It seems that the degree of overlapping yielding the optimum result is to be determined depending on particular application requirements. It is obvious, however, that the full potential of laser hardening cannot be realized over an extended surface when the technique of overlapping passes is used.

4. Summary

The effect of continuous CO_2 laser processing on the structure and hardness of AISI 1045 steel has been investigated in the cases of isolated and partially overlapping passes. The laser-affected region produced by an isolated pass consists of two distinct zones: (i) a melt zone, surrounded by (ii) an austenitization zone having a duplex structure representing former pearlite and ferrite regions. The hardness of the melt zone (about HV 750) exceeds that of conventionally hardened 1045 steel; an even higher hardness (up to HV 900) is observed in former pearlite regions of the austenitization zone, that of former ferrite regions being about HV 250. In the case of an extended surface processed by a series of equidistant passes, no essential changes are observed within the partially overlapping melt and austenitization zones. However, due to a heating effect produced by each pass in a previously hardened layer, a relatively wide region of tempered martensite is formed with minimum measured hardness values down to HV 400. As a result of this interaction the full potential of laser hardening cannot be realized when the technique of successive passes is used, and the surface layer thus formed shows a periodic hardness distribution pattern whose features depend on the degree of overlapping.

It has been also found that the use of a high-power beam can be counterproductive because a drastic decrease in the hardening depth occurs when the beam power density exceeds some threshold level.

Acknowledgements

The authors are grateful to Dr M. Bamberger for his help at the initial stage of the investigation and to Dr L. Zevin for X-ray diffraction measurements. This research was supported by a grant provided by the National Council for Research and Development, Israel, and the Directorate-General for Science Research and Development of the Commission of the European Community.

References

1. D. S. GNANAMUTHU, in Proceedings of Conference on Applications of Lasers in Materials Processing, Washington, DC, April 1979, edited by E. A. Meltzbower (ASM, Metals Park, Ohio, 1979) p. 177.
2. M. GARBUCICCHIO, G. MEAZZA, G. PALOMBARINI and G. SAMBOGNA, *J. Mater. Sci.* **18** (1983) 1543.
3. J. C. RAWERS, *ibid.* **20** (1985) 1929.
4. P. A. MOLIAN, *J. Mater. Sci. Eng.* **51** (1981) 253.
5. H. B. SINGH, S. M. COPLEY and M. BASS, *Met. Trans. A* **12** (1981) 138.
6. L. N. OBISHCHENKO, N. M. MIKHIN, D. A. DERGOBUZOV and S. N. PLATOVA, *Metallovedenie i termicheskaya obrabotka metallov (MiTOM)* (1983) No. 5, p. 18 (in Russian).
7. V. S. VELIKIH, V. P. GONCHARENKO, A. F. ZVEREV and V. S. KARTAVTSEV, *ibid.* (1985) No. 4, p. 9 (in Russian).
8. M. R. JAMES, D. S. GNANAMUTHU and R. J. MOORES, *Scripta Metall.* **18** (1984) 357.
9. M. LAMB, D. R. F. WEST and W. M. STEEN, *Mater. Sci. Tech.* **2** (1986) 974.
10. P. G. MOORE and L. S. WEINMANN, in "Laser Applications in Materials Processing", edited by J. F. Ready; *Proc. Soc. Photo-Opt. Instr. Eng.* **198** (1979) 120.
11. G. G. BORODINA, V. S. KRAPOSHIN, Yu. A. ROMANOV and F. K. KOSYREV, *Metallovedenie i termicheskaya obrabotka metallov (MiTOM)* (1983) No. 4, p. 14 (in Russian).
12. J. BENEDEK, A. SHACHRAI and L. LEVIN, *Opt. Laser Technol.* **12** (October 1980) 247.
13. J. F. READY, *Proc. IEEE* **70** (1982) 533.

Receiving 9 March
and accepted 2 June 1987